Cancer Immunol Immunother (2017) 66:1597–1608
DOI 10.1007/s00262-017-2052-5

ORIGINAL ARTICLE

# Interleukin 6 induces M2 macrophage differentiation by STAT3 activation that correlates with gastric cancer progression

**Xiao-Long Fu[1] · Wei Duan[1] · Chong-Yu Su[1] · Fang-Yuan Mao[2] · Yi-Ping Lv[2] · Yong-Sheng Teng[2] · Pei-Wu Yu[1] · Yuan Zhuang[2] · Yong-Liang Zhao[1]**

Received: 22 November 2016 / Accepted: 11 August 2017 / Published online: 21 August 2017


**Abstract** Interleukin 6 (IL-6) was abundant in the tumor microenvironment and played potential roles in tumor progression. In our study, the expression of IL-6 in tumor tissues from 36 gastric cancer (GC) patients was significantly higher than in non-tumor tissues. Moreover, the number of $CD163^+CD206^+$ M2 macrophages that infiltrated in tumor tissues was significantly greater than those infiltrated in non-tumor tissues. The frequencies of M2 macrophages were positively correlated with the IL-6 expression in GC tumors. We also found that IL-6 could induce normal macrophages to differentiate into M2 macrophages with higher IL-10 and TGF-β expression, and lower IL-12 expression, via activating STAT3 phosphorylation. Accordingly, knocking down STAT3 using small interfering RNA decreased the expression of M2 macrophages-related cytokines (IL-10 and TGF-β). Furthermore, supernatants from IL-6-induced M2 macrophages promote GC cell proliferation and migration. Moreover, IL-6 production and $CD163^+CD206^+$ M2 macrophage infiltration in tumors were associated with disease progression and reduced GC patient survival. In conclusion, our data indicate that IL-6 induces M2 macrophage differentiation ($IL\text{-}10^{high}TGF\text{-}\beta^{high}IL\text{-}12_{p35}^{low}$) by activating STAT3 phosphorylation, and the IL-6-induced M2 macrophages exert a pro-tumor function by promoting GC cell proliferation and migration.

**Keywords** Gastric cancer · IL-6 · STAT3 · M2 macrophages · Tumor progression

**Abbreviations**

| | |
|---|---|
| Bcl-xL | B-cell lymphoma-extra large |
| CCK8 | Cell counting kit 8 |
| CCL2 | Chemokine (C–C motif) ligand 2 |
| GC | Gastric cancer |
| M-CSF | Macrophage colony-stimulating factor |
| PBMC | Peripheral blood mononuclear cell |
| p-STAT3 | Phosphorylated STAT3 |
| PVDF | Polyvinylidene difluoride |
| SEM | Standard error of mean |
| siRNA | Small interfering RNA |
| SOCS3 | Suppressor of cytokine signaling 3 |
| TAMs | Tumor-associated macrophages |
| TBST | Tris-buffered saline with Tween-20 |
| VEGF | Vascular endothelial growth factor |

## Introduction

Macrophages are a heterogeneous cell population in the immunologic system that plays a significant role in our body's defense against bacterial, viral, and parasitic infection. Macrophages that infiltrate the tumor microenvironment are called tumor-associated macrophages (TAMs).

**Electronic supplementary material** The online version of this article (doi:10.1007/s00262-017-2052-5) contains supplementary material, which is available to authorized users.

✉ Yuan Zhuang
yuanzhuang1983@yahoo.com

✉ Yong-Liang Zhao
yongliang1666@163.com

[1] Department of General Surgery and Center of Minimal Invasive Gastrointestinal Surgery, Southwest Hospital, Third Military Medical University, No. 30 Gaotanyan Street, Chongqing 400038, People's Republic of China

[2] National Engineering Research Centre of Immunological Products, Department of Microbiology and Biochemical Pharmacy, College of Pharmacy, Third Military Medical University, No. 30 Gaotanyan Street, Chongqing 400038, People's Republic of China

TAMs are derived from circulating monocytes recruited locally by chemokine (C–C motif) ligand 2 (CCL2), macrophage colony-stimulating factor (M-CSF), and vascular endothelial growth factor (VEGF) [1]. LPS or IFN-γ can induce macrophage differentiation to M1 (classically activated) macrophages [2, 3]. IL-4 and IL-13 promote macrophage polarization to an M2 type (alternatively activated) [2]. M1 macrophages are potent effector cells that kill microorganisms and primarily produce pro-inflammatory cytokines, such as tumor necrosis factor-α (TNF-α) and IL-12 [4], and are essential for clearing bacterial, viral, and fungal infections [5]. However, M2 macrophages suppress these inflammatory and adaptive Th1 responses by producing anti-inflammatory factors [such as IL-10 and transforming growth factor-β (TGF-β)] [3, 6]. M2 macrophages also play a significant role in responses to parasitic infection, tissue remodeling, angiogenesis, and tumor progression [7] and present an IL-$12^{low}$IL-$10^{high}$ phenotype [8, 9]. However, the regulatory mechanisms by which M2 macrophage differentiation occurs and their relevance to human gastric cancer (GC) are yet to be elucidated.

IL-6 has a dual function in the immune system: it exerts a pro-inflammatory [10] or an anti-inflammatory [11] effect dependent on the local immune microenvironment. IL-6 is pleiotropic because of its hormone-like attribute that affects vascular disease, lipid metabolism, insulin resistance [12], and neuropsychological behavior [13]. IL-6 is known as a strong activator of STAT3, the activated, phosphorylated STAT3 (p-STAT3) rapidly translocates into the nucleus, and binds to a recognition sequence in the promoter of target genes including Cyclin D1, B-cell lymphoma-extra large (Bcl-xL) c-Myc, and VEGF [14], thereby increasing the transcription and expression of these target genes. IL-6-dependent STAT3 activation plays a pivotal role in tumor progression such as breast cancer [15], colorectal cancer [16], and head and neck cancer [17]. IL-6-stimulated macrophages showed a robust increased expression of IL-10. IL-6 induces STAT3 to bind to IL-4Ra promoter, therefore, promoting IL-4-dependent activation of STAT6 [11]. IL-4-STAT6 pathway regulates macrophage polarization by inducing M2-associated genes such as mannose receptor 1 (Mrc1), arginase 1(Arg1), IL-10, and resistin-like alpha (Retnla) [18]. Moreover, it was demonstrated that myeloid cell-specific disruption of suppressor of cytokine signaling 3 (SOCS3), the negative regulator of the IL-6-STAT3 axis, skews macrophages towards an M2 phenotype [19]. The mechanism and associated clinical relevance of IL-6-STAT3 pathway in M2 macrophage differentiation in GC are not yet elucidated in humans.

In the present study, we showed that IL-6 expression in the tumor tissues of GC patients was higher than in the non-tumor tissues. Moreover, the number of $CD163^+CD206^+$ M2 macrophages infiltrating GC tumors was also increased. The number of $CD163^+CD206^+$ M2 macrophages was positively correlated with IL-6 production in GC. We also found that IL-6 could induce normal macrophages to differentiate into M2 macrophages that had a phenotype that induced higher IL-10 and TGF-β expression and lower IL-$12_{p35}$ expression via activating STAT3 phosphorylation. The supernatants from IL-6-induced M2 macrophages promoted gastric cancer cell proliferation and migration. Therefore, our data indicate that IL-6 induces M2 macrophage differentiation (IL-$10^{high}$TGF-$\beta^{high}$IL-$12^{low}_{p35}$) by activating STAT3 phosphorylation, and the IL-6-induced M2 macrophages exert a pro-tumor function by promoting GC cell proliferation and migration.

## Materials and methods

### Patients and tissue samples

Tumor and non-tumor (at least 5 cm from the tumor site, no cancer cell infiltration as confirmed by histopathology) gastric tissues were obtained from patients who underwent surgical resection at the Southwest Hospital of the Third Military Medical University. None of the patients had received radiotherapy or chemotherapy before sampling. The clinical stages of tumors were determined according to the TNM classification system of the International Union Against Cancer (Edition 7). The study was approved by the Ethics Committee of the Southwest Hospital of the Third Military Medical University. Written informed consent was obtained from each subject.

### Immunohistochemistry

For immunohistochemistry, paraffin-embedded samples of GC tissues were cut into 4-μm sections. Sections were pre-incubated with normal goat serum at 37 °C for 30 min followed by incubation with primary mouse anti-IL-6 antibody (Abcam, Cambridge, MA, USA) or anti-CD163 rabbit monoclonal antibody (Abcam) overnight at 4 °C, and then incubated with horseradish peroxidase (HRP-) conjugated anti-mouse or anti-rabbit secondary antibody (Zhongshan Biotechnology, Beijing, China) at 37 °C for 30 min. Polink DS-MR-Hu A2 Kit (Zhongshan Biotechnology) was used for double staining of CD163 and CD206 with anti-CD163 rabbit antibody and anti-CD206 mouse antibody (Abcam) according to the manufacturer's instructions. All sections were analyzed independently by two experienced pathologists who did not have access to the clinical data of patients. Five fields were observed in each section, and the cells with uniform brown granules were counted at 200× magnification in each case using average values.

### ELISA analysis

Tumor and non-tumor tissues from specimens were collected; the total protein was extracted with 1 ml RIPA Lysis and Extraction Buffer (Pierce, Rockford, USA) and centrifuged. Concentrations of cytokine in the tissue supernatants were determined using ELISA kits for IL-6 [20] (eBioscience, CA, USA); concentrations of cytokine in the cell culture supernatants were determined using ELISA kits for IL-10 (eBioscience) and TGF-β (eBioscience) according to the manufacturer's instructions.

### Cell isolated and M2 macrophage induction

Human peripheral blood mononuclear cells (PBMCs) were separated from fresh blood samples from healthy donors by density gradient centrifugation using Ficoll-Hypaque (GE Healthcare, NJ, USA). $CD14^+$ monocytes were isolated from PBMCs using a Human CD14 Positive Selection Kit (Stem Cell Technologies, Vancouver, Canada) according to the manufacturer's instructions. Then, the purity of monocytes was measured by flow cytometry. Cells were cultured in a 12-well plate with $5 \times 10^5$ per well and were induced to differentiate to normal macrophages (M0) with M-CSF (PeproTech, NJ, USA) for 5 days with a final concentration of 100 ng/ml. On day 6, human recombinant IL-6 (50, 100, and 200 ng/ml) (Pepro Tech, NJ, USA) was added to induce M0 macrophages (purity of M0 macrophages was 60–70%, data not shown) to differentiate into M2 macrophages for a period of 24 h. All cells were cultured at 37 °C in a humidified incubator with 5% $CO_2$.

### Immunofluorescence

M0/M2 macrophages ($5 \times 10^5$ per well) were induced as described above. Cells were washed in PBS and blocked for 30 min with 20% goat serum in PBS, and then incubated with rabbit anti-human p-STAT3 antibody (Cell Signaling Technology, MA, USA) diluted in 5% goat serum. The bound antibody was detected with tetramethylrhodamine conjugated goat anti-rabbit antibody (Zhongshan Biotechnology). After washing with PBS, cells were examined with a fluorescence microscope.

### Transfection of macrophages with siRNA

M0 macrophages ($5 \times 10^5$ per well) were induced as described above and were transfected with either STAT3 targeting or non-silencing control siRNA with a final concentration of 40 pmol/ml, according to the manufacturer's recommendations (GenePharma, Shanghai, China). After a 6-h transfection, the cells were further cultured in fresh RPMI-1640 medium supplemented with 10% FBS and M-CSF (100 ng/ml) for 24 h. After this culture period, cells were induced to differentiate to M2 macrophages in the presence of IL-6 (100 ng/ml) for 24 h.

### Quantitative RT-PCR

Total RNA was extracted from cultured cells using Trizol reagent according to the manufacturers' instructions (Invitrogen). The RNA (500 ng in 10 µl volume) was reverse transcribed with a reverse transcription kit (Takara, Otsu, Japan). cDNA was obtained and diluted with 10 µl nuclease free water. Real-time PCR was performed on a BIO-RAD CFX96-Tm Real-Time System by mixing 2 µl cDNA with SYBR Green Master Mix (Applied Biosystems, USA), using the following forward and reverse primers (GenePharma, Shanghai, China): human IL-10 (forward 5′-GCTGTCATC GATTTCTTCCC-3′, reverse 5′-CTCATGGCTTTGTAG ATGCCT-3′, 103 bp); IL-12 (forward 5′-AGGGCCGTC AGCAACATG-3′, reverse 5′-TCTTCAGAAGTGCAA GGGTAAAATTC-3′, 68 bp); TGF-β (forward 5′-AACTAC TGCTTCAGCTCCAC-3′, reverse 5′-TGTGTCCAGGCT CCAAATGTA-3′, 155 bp); CD163 (forward 5′-CGAGTT AACGCCAGTAAGG-3′, reverse 5′-GAACATGTCACG CCAGC-3′, 146 bp); CD206 (forward 5′-CGAGGAAGA GGTTCGGTTCACC-3′, reverse 5′-GCAATCCCGGTT CTCATGGC-3′, 84 bp); STAT3 (forward 5′-GGGTGG CGAAGGACATCAGCGGTAA-3′, reverse 5′-GCCGAC AATACTTTCCGAATGC-3′, 198 bp); and β-actin (forward 5′-GGCATCGTGATGGACTCCG-3′, reverse 5′-GCTGGA AGGTGGACAGCGA-3′, 613 bp). The relative expression of target mRNAs was calculated using the $2^{-\Delta\Delta CT}$ method (using β-actin as a calibrator).

### Western blot analysis

The total protein was extracted by RIPA Lysis and Extraction Buffer (Pierce) with protease and phosphatase inhibitors (Roche, Basel, Switzerland) according to the manufacturer's protocol. Protein samples (10 µg) boiled with SDS-PAGE loading buffer were separated by 10% SDS–polyacrylamide gels, and then proteins were transferred to PVDF (polyvinylidene difluoride) membranes (Millipore, Bedford, MA, USA). The membranes were incubated with primary antibodies against STAT3 (1:500; Santa Cruz Biotechnology, CA, USA), p-STAT3 (phospho-Tyr705) (1:1000; CST), and β-actin (1:000; Santa) overnight at 4 °C, respectively, and then incubated with horseradish peroxidase (HRP)-conjugated secondary antibodies (diluted 1:10,000 in 3% BSA blocking buffer) (Zhongshan Biotechnology) for 45 min at room temperature. After washed in TBST (Tris-buffered saline with Tween-20), the membranes were incubated with SuperSignal™ West Dura Extended Duration Substrate

(Thermo Scientific™) for 1 min. The blots were analyzed using chemiluminescence.

### Collection of supernatants

M0 macrophages were induced as described above. On day 6, for M0 macrophage group, cells were cultured for 24 h without IL-6; for the M2 macrophage group, IL-6 (100 ng/ml) was added to induce the macrophage differentiation to M2 macrophages for 24 h. Then, the medium for both M0 and M2 macrophage groups was exchanged with 400 µl fresh RPMI-1640 (10% FBS) medium per well; cell-free supernatants from M0 or M2 macrophage group were harvested after another 24-h culture.

### Cell proliferation and migration analysis

For cell proliferation, $5 \times 10^3$ cells per well of GC cell lines (AGS and SGC-7901) were co-cultured with M2 macrophage supernatants (100%) with or without antibodies against IL-10 (10 µg/ml) (Biolegend, San Diego, CA, USA) or TGF-β (10 µg/ml) (Abcam) in 96-well plates. The OD values were measured at 24, 48, and 72 h with a Cell Counting Kit 8 (CCK8) (DOJINDO, Tokyo, Japan) according to the manufacturer's instructions. Cell migration was analyzed using a 24-well plate that contained transwell inserts (Corning, MA, USA). The AGS or SGC-7901 cells were suspended in serum-free RPMI-1640 medium, and $1 \times 10^5$ of these cells were seeded per insert. Then, 600 µl of the M2 macrophage supernatants with or without antibodies against IL-10 (10 µg/ml) or TGF-β (10 µg/ml) were added to the lower chamber of the corresponding groups and incubated at 37 °C. After 24 h, migrated cells on the lower surface of the membrane were stained, and cells were counted in five fields of vision and photographed under microscopy at 200 × magnification.

### Statistical analysis

Results are expressed as the mean ± SEM (standard error of mean). The statistical significance of the differences between the two groups was determined by Student's *t* test. ANOVA was performed for multi-group data analysis. Correlations between parameters were assessed using the Pearson correlation analysis and linear regression analysis, as appropriate. Overall patient survival was defined as the interval between the date of surgery and the date of death or last follow-up, whichever occurred earlier. The known tumor-unrelated deaths (e.g., intercurrent disease and accidental death) were excluded from the death record for this study. Cumulative survival time was calculated by the Kaplan–Meier method, and survival was measured in months; the log-rank test was applied for comparison between two groups. SPSS statistical software (version 13.0) was used for all statistical analyses. All data were analyzed using two-tailed tests, and $p < 0.05$ was considered statistically significant unless otherwise specified.

## Results

### Patients' characteristics

A total of 36 never-treated GC patients were collected from March 2014 to August 2015. The baseline clinical and pathological characteristics are presented in Supplementary Table 1.

### M2 macrophage infiltration and IL-6 production are enhanced with close correlation in GC

Using immunohistochemistry, we first evaluated IL-6 expression between tumor and non-tumor tissues of GC patients. IL-6 expression was significantly higher in tumor tissues compared with non-tumor tissues (Fig. 1a). To further verify this result, we assessed IL-6 production by ELISA, and the results showed that IL-6 production in tumor tissues (44.82 ± 19.95 pg/mg) was significantly higher than that in non-tumor tissues (26.67 ± 13.80 pg/mg) ($p < 0.01$) (Fig. 1b).

The immunohistochemical staining for $CD163^+$ macrophage and $CD163^+CD206^+$ M2 macrophage infiltration also showed their significantly increased infiltration into tumor tissues (Fig. 1c, e). Statistical analysis showed that the number of $CD163^+$ macrophages (34.81 ± 15.29 cells/field) (Fig. 1d) and $CD163^+CD206^+$ M2 macrophages (16.22 ± 6.91 cells/field) (Fig. 1f) in tumor tissues were significantly higher than that in non-tumor tissues (3.19 ± 2.04 and 1.47 ± 1.23 cells/field), respectively ($p < 0.01$). Further analysis showed that the number of $CD163^+$ macrophages was positively correlated with IL-6 production ($N = 36$, $R^2 = 0.6407$, $p < 0.01$) (Fig. 1d). Moreover, $CD163^+CD206^+$ M2 macrophages were also positively correlated with IL-6 production ($N = 36$, $R^2 = 0.4300$, $p < 0.01$) (Fig. 1f). Therefore, our data indicate that M2 macrophage infiltration and IL-6 production are enhanced and positively correlated in GC.

### IL-6 induces M2 macrophage differentiation

IL-6 production and its correlation with increased local M2 macrophage infiltration increased in GC tumors (Fig. 1e, f); therefore, we stimulated the M-CSF-induced M0 macrophages with different concentrations of IL-6 to investigate whether this stimulation was capable of inducing the differentiation of M0-to-M2 macrophages. After a 24-h

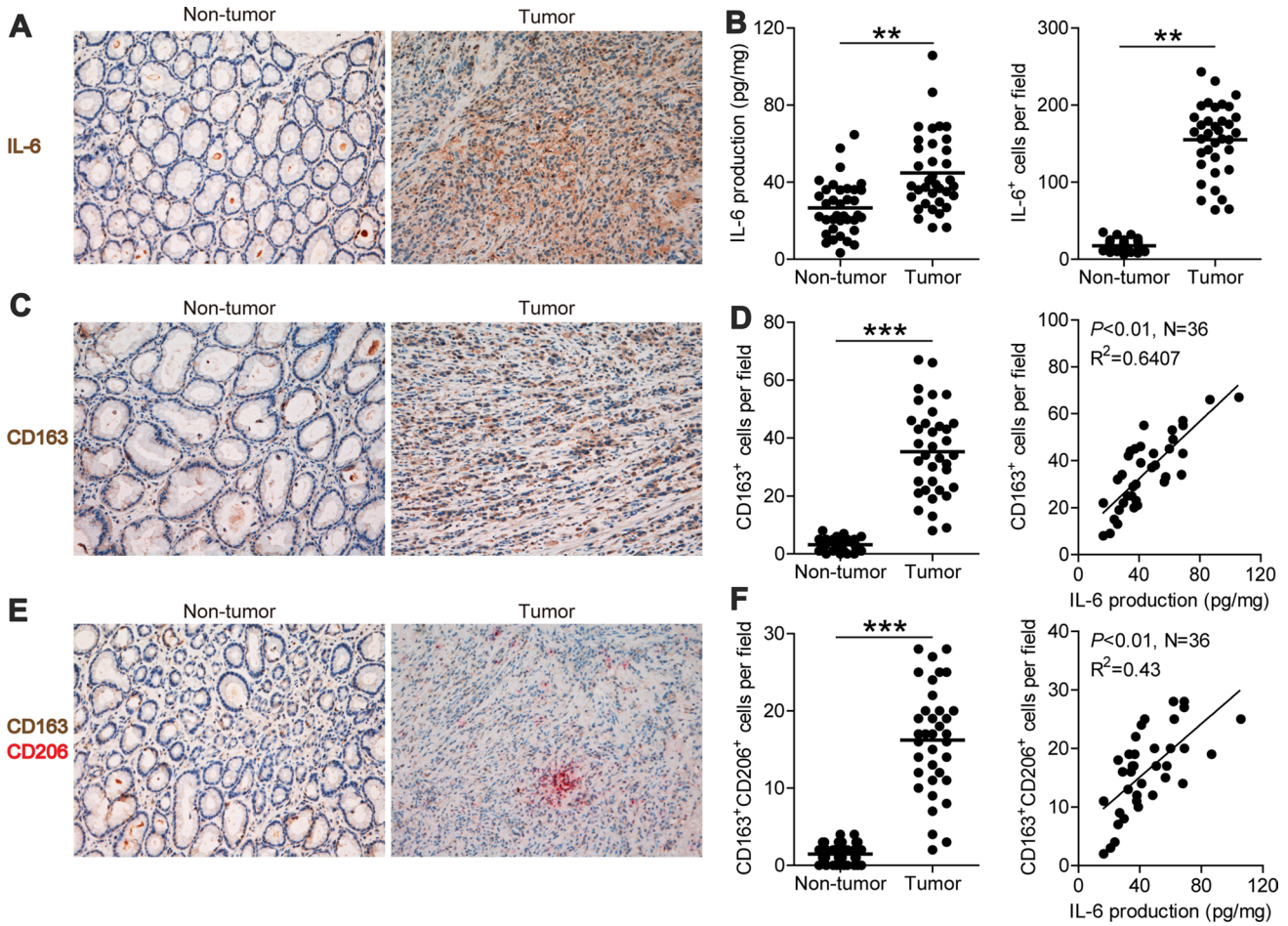


**Fig. 1** Expression of IL-6 and distribution of $CD163^+CD206^+$ M2 macrophages in gastric tumor and non-tumor tissues. **a** Representative images of $IL\text{-}6^+$ cell (*brown*) in non-tumor and tumor tissues; images were taken at ×200 magnification. **b** Expression of IL-6 in tumor and non-tumor tissues was determined using ELISA; $IL\text{-}6^+$ cells infiltrating tumor and non-tumor tissues were counted and analyzed, and the data are presented as the mean ± SEM, $^{**}p < 0.01$. **c** Representative images of $CD163^+$ macrophages (*brown*) in non-tumor and tumor tissues; images were taken at ×200 magnification. **d** $CD163^+$ macrophages infiltrating tumor and non-tumor tissues were counted and analyzed; the data are presented as the mean ± SEM, $^{**}p < 0.01$; the correlation of infiltrated $CD163^+$ macrophages and IL-6 production in gastric tumor tissues; $N = 36$, $R^2 = 0.641$, $p < 0.01$. **e** Representative images of $CD163^+CD206^+$ M2 macrophages in non-tumor and tumor tissues; images were taken at ×200 magnification. **f** $CD163^+CD206^+$ M2 macrophages infiltrating tumor and non-tumor tissues were counted and analyzed; the data are presented as the mean ± SEM, $^{**}p < 0.01$; the correlation of infiltrated $CD163^+CD206^+$ M2 macrophages and IL-6 production in gastric tumor tissues; $N = 36$, $R^2 = 0.43$, $p < 0.01$

stimulation, the total RNA was extracted, and RT-PCR was applied to identify the M2 macrophage markers (IL-10, TGF-β, and CD206). The results showed that the expression of IL-10, TGF-β, and CD206 increased along with the increased concentration of IL-6 (Fig. 2a–c). Moreover, the expression of M1 macrophage marker $IL\text{-}12_{p35}$ decreased along with the increased concentration of IL-6 (Fig. 2f). To further identify this, we detected the concentrations of IL-10 and TGF-β in the cell culture supernatants by ELISA. Results showed that both the IL-10 and TGF-β productions raised with the increased concentration of IL-6 (Fig. 2d, e). These data indicate that IL-6 induces the polarization of M0 macrophages to M2 macrophages ($IL\text{-}10^{high}TGF\text{-}\beta^{high}IL\text{-}12^{low}_{p35}$) in a dose-dependent manner.

## IL-6 induces macrophage STAT3 phosphorylation

To investigate the underlying mechanism of how IL-6 induces M2 macrophage differentiation, we focused on the IL-6-induced downstream STAT3. After IL-6 stimulation, the total RNA and total protein of macrophages were extracted, and RT-PCR was used to determine the STAT3 gene transcription level. Our results showed that increasing IL-6 stimulation did not significantly increase the total STAT3 expression in macrophages at the gene level (data not shown). Next, we determined the protein levels of total STAT3 and activated p-STAT3 by Western blot and found that the total STAT3 protein levels remain unchanged, but the activated p-STAT3 protein levels were significantly

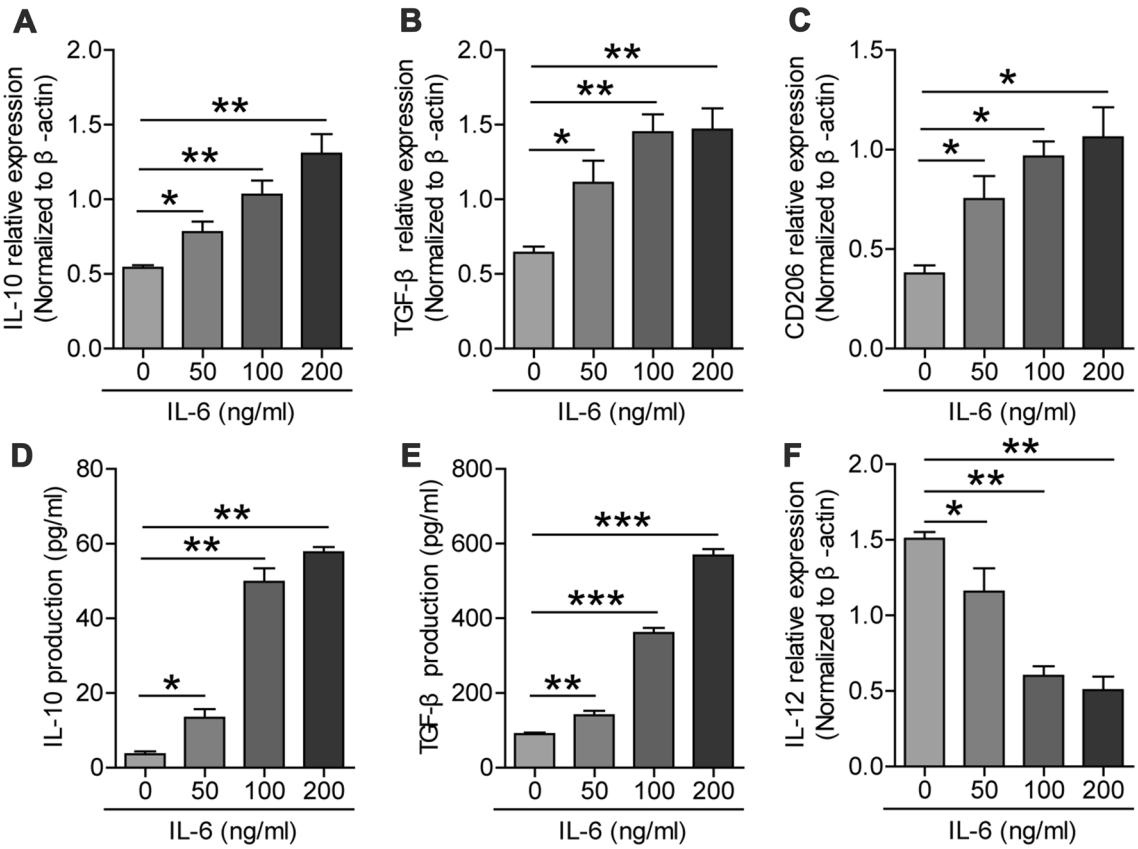


**Fig. 2** Expression of IL-10, TGF-β, CD206, and IL-$12_{p35}$ in IL-6-induced macrophages. **a** Relative expression of IL-10 increased with the increasing IL-6 dose. **b** Relative expression of TGF-β increased with the increasing IL-6 dose. **c** Relative expression of CD206 increased with the increasing IL-6 dose. **d** Production of IL-10 in the cell culture supernatants increased with the increasing IL-6 dose. **e** Production of TGF-β in the cell culture supernatants increased with the increasing IL-6 dose. **f** Relative expression of IL-12 decreased with the increasing IL-6 dose; $*p < 0.05$, $**p < 0.01$ compared to the control (0 ng/ml)

increased with increasing IL-6 concentration (Fig. 3a, b). The immunofluorescence results corroborated this result and showed that the activated p-STAT3 level in the IL-6-induced M2 macrophages was significantly higher than that of the controls (Fig. 3c, d). Moreover, the p-STAT3 in M2 macrophages was primarily localized in the nucleus (Fig. 3c). Taken together, these results indicate that the STAT3 signaling pathway is significantly activated during the process of IL-6-induced M2 macrophage differentiation.

### IL-6 induces M2 macrophage differentiation via STAT3 phosphorylation

To further examine the regulatory role of the p-STAT3 in IL-6-induced M2 macrophage differentiation, we used siRNA to pre-interfere with STAT3 expression. We then repeated the IL-6-induced M2-type macrophage differentiation test. The results showed that the gene expression (Fig. 4a) and protein production (Fig. 4b) of STAT3 were significantly knocked down compared with control siRNA and control groups. Notably, we also found that the p-STAT3 protein level decreased in the STAT3 siRNA-treated group compared with control siRNA and control groups (Fig. 4b). These results confirmed that siRNA significantly inhibits the expression of total STAT3, thereby decreasing the level of phosphorylated STAT3 when IL-6 added.

To further clarify whether the down-regulation of p-STAT3 expression was crucial for the IL-6-induced M2 macrophage differentiation, the expression of IL-10, TGF-β, CD206, and IL-$12_{p35}$ was analyzed. The expression of IL-10, TGF-β, and CD206 significantly decreased in the STAT3 siRNA group compared with control siRNA and control groups when IL-6 was added. The IL-10 and TGF-β production in the cell culture supernatant also decreased in the STAT3 siRNA group when IL-6 was added (Fig. 4d). Moreover, the expression of IL-$12_{p35}$ increased in the STAT3 siRNA group (Fig. 4c). Taken together, these data indicated that IL-6 induces M2 macrophage differentiation with the IL-$10^{high}$TGF-$\beta^{high}$IL-$12^{low}_{p35}$ phenotype via STAT3 phosphorylation.

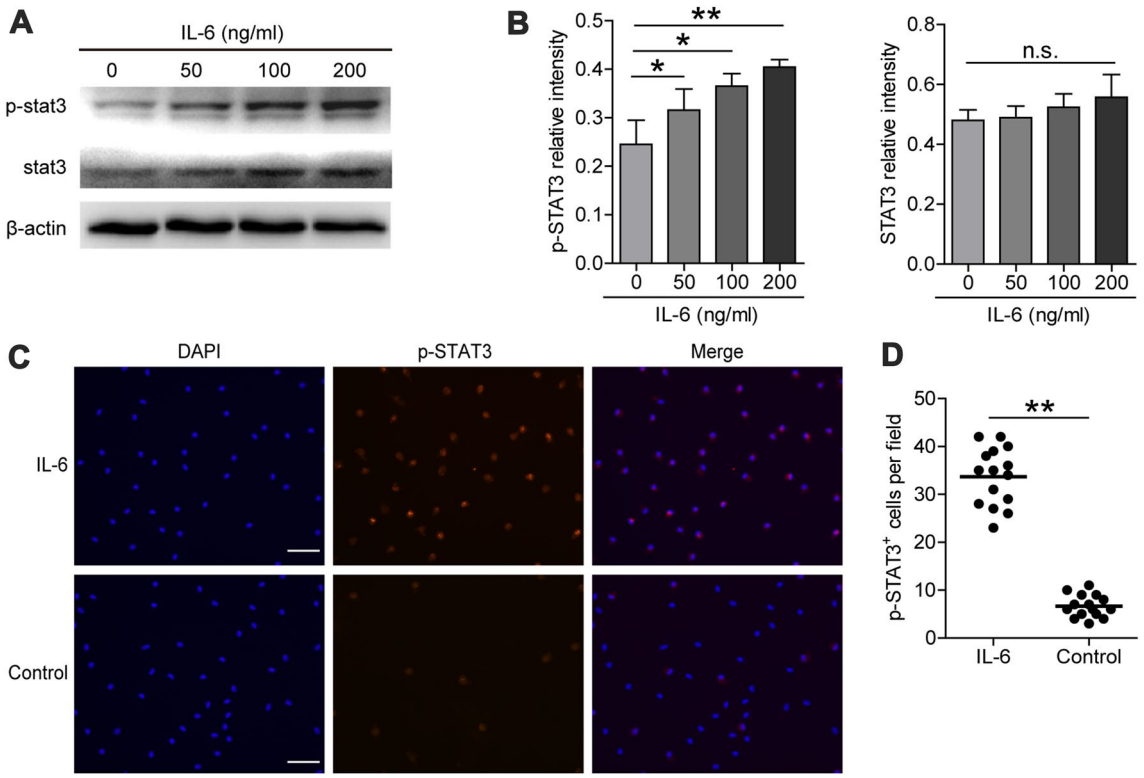


**Fig. 3** Expression of STAT3 and p-STAT3 in IL-6-induced M2 macrophages. **a** Total STAT3 protein and p-STAT3 protein levels were determined with western blot, and β-actin was used as a reference control. **b** Relative intensity of total STAT3 protein and p-STAT3 protein. **c** Immunofluorescence staining for IL-6 (100 ng/ml) induced M2 macrophages (*Scale bar* 200 μm). The *red signal* represents the staining of activated p-STAT3, and the blue signal represents the DAPI-stained nuclei. **d** p-STAT3$^+$ cells in IL-6(100 ng/ml) and control group were counted and analyzed, data are presented as the mean ± SEM; $*p < 0.05$, $**p < 0.01$, *n.s.* indicates $p > 0.05$ for groups connected by *horizontal lines* compared in **b**

### Supernatants from IL-6-induced M2 macrophages promote GC cell proliferation and migration

To investigate the functions of IL-6-induced macrophages, we collected the supernatants from IL-6-induced M2 macrophages and studied the effect of these supernatants on the proliferation and migration of GC cells (AGS and SGC-7901).

First, for proliferation analysis, GC cell lines were co-cultured with M2 macrophage supernatants with or without antibodies against IL-10 or TGF-β; the $OD_{450}$ values were determined with a CCK8 proliferation assay kit. The $OD_{450}$ value at 72 h for the GC cells in M2 macrophage supernatants group (AGS 1.25 ± 0.12; SGC 1.33 ± 0.14) was significantly higher than that in the RPMI-1640 control group (AGS 0.90 ± 0.02; SGC 0.98 ± 0.07) (Fig. 5a, b). Moreover, the pro-proliferation effect of M2 macrophage supernatants was attenuated in the presence of IL-10 or TGF-β antibodies (Fig. 5a, b).

Next, for migration analysis, GC cell lines were co-cultured with M2 macrophage supernatants with or without antibodies against IL-10 or TGF-β. The migration abilities of the GC cells co-cultured with different supernatants were evaluated with the statistics counts of cancer cells that permeated the basement membrane. For the AGS cell line, the number of the migrated cells in the M2 macrophage supernatant group (257.6 ± 6.26) was higher than that in the RPMI-1640 medium group (187.8 ± 6.09) (Fig. 5c, e). For the SGC cell line, the number of migrated cells in the M2 macrophage supernatants group (218.6 ± 4.62) was also higher than that in the RPMI-1640 medium group (152.0 ± 7.91) (Fig. 5d, f). Meanwhile, the pro-migration effect of M2 macrophage supernatants was attenuated by blocking IL-10 or TGF-β with neutralizing antibodies. Taken together, these data indicate that IL-6-induced M2 macrophages release soluble factors (IL-10 and TGF-β) to promote GC cell proliferation and migration.

### Enriched IL-6 and M2 macrophages are correlated with the tumor stage and survival in patients with GC

Finally, we studied whether increased IL-6 production and M2 macrophage infiltration were associated with the tumor stage and GC patient survival. We observed that IL-6

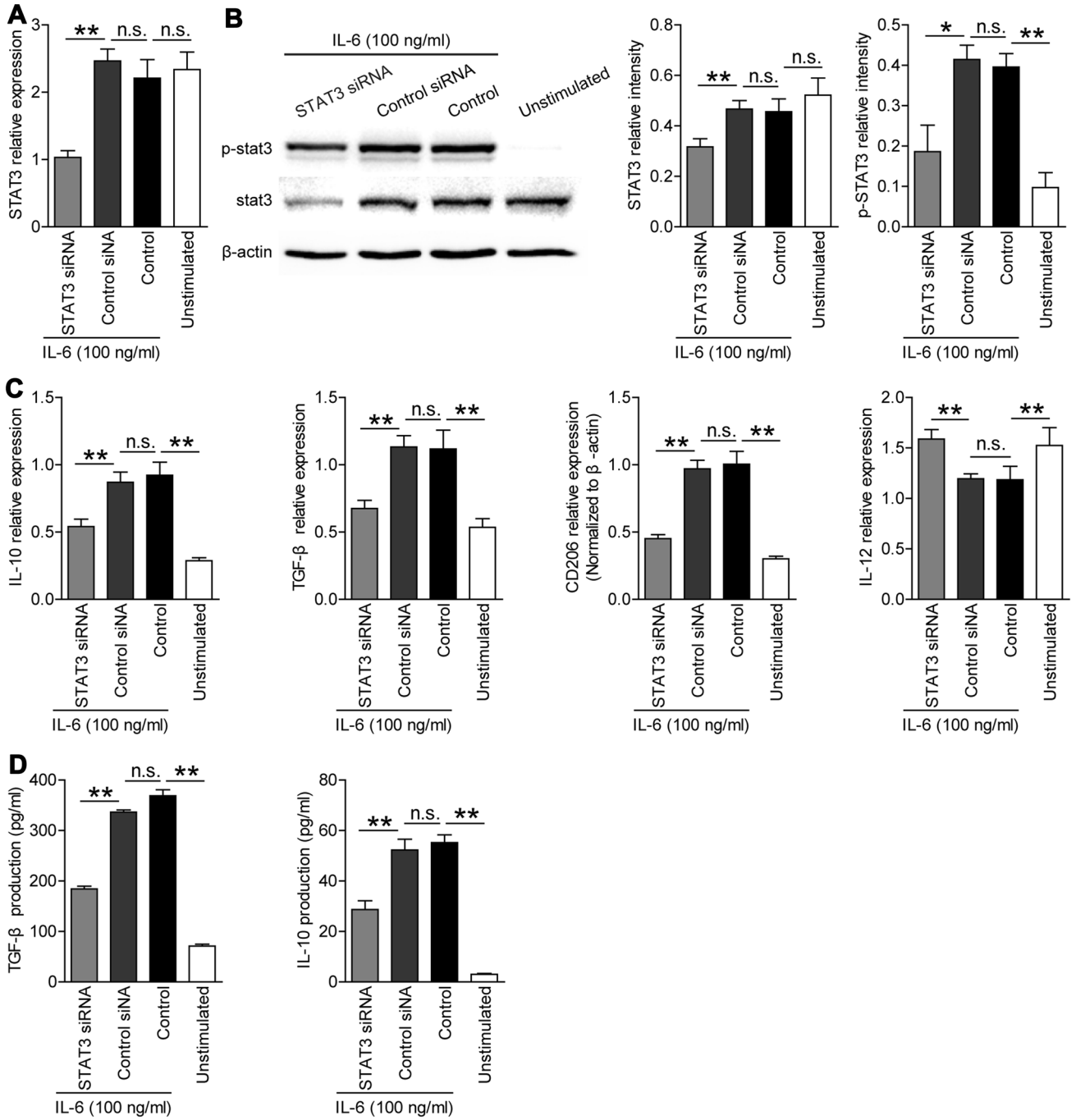


**Fig. 4** Expression of IL-10, IL-$12_{p35,}$ and TGF-β in IL-6-induced M2 macrophages with or without knocking down STAT3 gene. **a** STAT3 gene expression was knocked down (depressed) with siRNA, and the silence efficiency was determined with RT-PCR. **b** STAT3 and p-STAT3 protein levels in the siRNA group and the normal induced M2 group were determined by western blot; relative intensity of STAT3 and p-STAT3 were analyzed. **c** Expression of IL-10, TGF-β, CD206, and IL-$12_{p35}$ in the siRNA group and the normal induced M2 group was determined using RT-PCR. **d** Production of IL-10 and TGF-β in the cell culture supernatants of the siRNA group and the normal induced M2 group were determined using ELISA (*$p < 0.05$, **$p < 0.01$, *n.s.* indicates $p > 0.05$ for groups connected by *horizontal lines*)

production increased with the advancement in tumor stage (Fig. 6a). The number of infiltrated M2 macrophages in GC tumors also increased with tumor progression (Fig. 6b).

Moreover, we assessed the relationship between increased IL-6 production or M2 macrophage infiltration and the survival of GC patients. The median values of IL-6 production

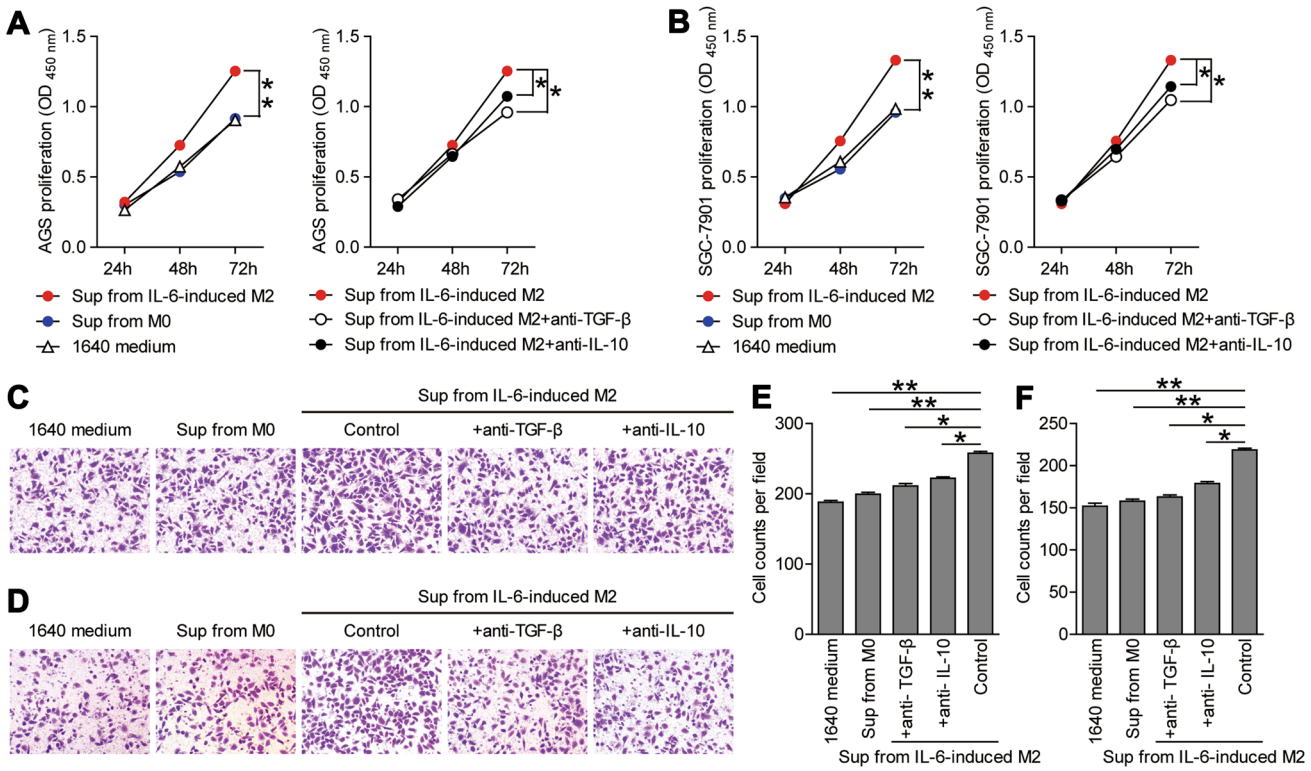


**Fig. 5** Supernatants from IL-6-induced M2 macrophages promote GC cell proliferation and migration. The proliferation of AGS (**a**) and SGC-7901 (**b**) GC cells co-cultured with the supernatants from M2-type macrophages with or without antibodies for IL-10 or TGF-β, and $OD_{450}$ values were measured to evaluate the proliferation. $OD_{450}$ values are presented as the mean ± SEM, $n = 5$, $p < 0.05$. **c**, **d** Migration abilities of the GC cells co-cultured with supernatants from M2-type macrophages with or without antibodies for IL-10 or TGF-β were evaluated with the statistical counts of cancer cells that permeated the basement membrane. Representative images (×200 magnification) of the migration of AGS GC cells (**c**), and the numbers of migrated cells are presented as the mean ± SEM (**e**). Representative images (×200 magnification) of the migration of SGC-7901 GC cells (**d**), and the numbers of migrated cells are presented as the mean ± SEM (**f**) ($n = 5$, $^*p < 0.05$, $^{**}p < 0.001$.)

and M2 macrophage density were used as cut-off points to divide the patients into a low group or high group. Further association of M2 macrophage and IL-6 production with survival was assayed using Kaplan–Meier survival curves. Comparing patients with high (above median level) versus low (below median level) IL-6 production, the 2-year survival rate was significantly higher for those with the lower IL-6 production ($p < 0.05$) (Fig. 6c). Moreover, the 2-year survival rate of GC patients with higher M2 macrophage density group was significantly lower than those with lower M2 macrophage density ($p < 0.05$) (Fig. 6d). Taken together, these data indicate that enriched IL-6 and M2 macrophages are correlated with tumor stage and survival in patients with GC.

## Discussion

Macrophages act as versatile cells, because they can differentiate into many subsets in response to the cytokine milieu. Interleukin 6 has a broad effect on both cells in the immune system and those not in the immune system [21]. Tumor-associated leukemia inhibitory factor and IL-6 skew monocyte differentiate into tumor-associated macrophage-like cells by enabling autocrine/paracrine M-CSF consumption [22]. Previously reported results demonstrated that M-CSF favored monocyte recruitment at the tumor site and murine TAM survival [23, 24]. The IL-6-induced macrophages present increased IL-10 mRNA expression and decreased IL-$12_{p35}$ and IL-$23_{p19}$ mRNA after LPS stimulation [22]. IL-6 can stimulate IL-10 expression and release. Both IL-10 [25] and IL-6 [11] can directly induce IL-4R gene expression in macrophages, and thus, promote macrophages differentiate into M2 macrophages in an IL-4-dependent manner. High level of TAM infiltration is related to aggressive features and is an independent prognostic factor in gastric cancer [26]. In this study, we found that IL-6 was highly expressed in tumor tissues. Our data showed that tumors with a high production of IL-6 also have a high density of $CD163^+$ macrophages ($R^2 = 0.6407$) and $CD163^+CD206^+$ M2 macrophages ($R^2 = 0.4300$). Thus, we can conclude that the high IL-6 expression at the tumor site was closely related to

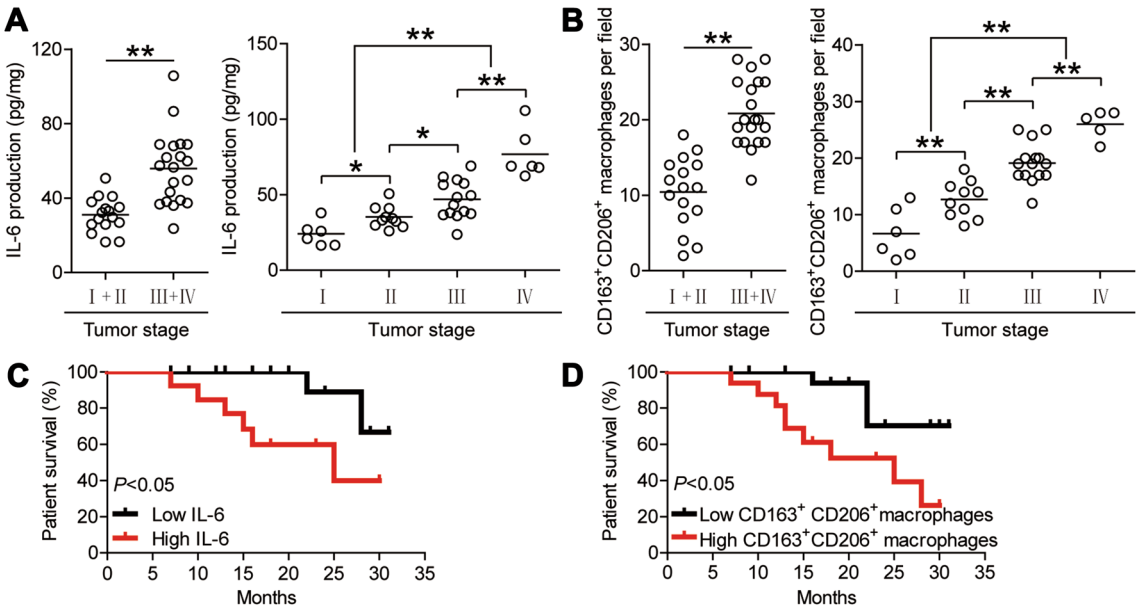


**Fig. 6** IL-6 and M2 macrophages are enriched in tumors and correlate with tumor stage and survival in GC patients. **a** Correlation of the production of IL-6 in tumor tissues and TNM stage was compared, combined or separated. **b** Numbers of $CD163^+CD206^+$ macrophages per field in TNM stages were compared, combined or separated. **c** Kaplan–Meier curve for overall survival with median IL-6 concentration. Survival significantly decreased as a function of the increasing concentration of IL-6. **d** Kaplan–Meier curve for overall survival with the median $CD163^+CD206^+$ macrophage number per field. Survival significantly decreased as a function of the increasing number of $CD163^+CD206^+$ macrophages. The *horizontal bars* in **a** and **b** represent mean values. *Each ring* (in **a** and **b**) represents one patient

macrophage accumulation and M2 macrophage differentiation in gastric cancer.

To elucidate the underlying mechanism of IL-6-induced macrophage differentiation, we built a differentiation system using IL-6 to stimulate the macrophages in vitro. The activation of STAT3 contributed to M2 macrophage polarization reported in many cancers [27–29], but it was not investigated in gastric cancers. The measurement of the STAT3 and phosphorylated STAT3 levels in the macrophages stimulated by different concentrations of IL-6 showed that the expression of total STAT3 was not changed, but the level of phosphorylated STAT3 was significantly increased with the increase in IL-6 concentration. This result indicated that STAT3 activation occurs in an IL-6-dose-dependent manner. It is accepted that IL-10 and TGF-β are mainly produced by M2-polarlized macrophages [30]. Our study showed that IL-6-induced macrophages tend toward $IL\text{-}10^{high}TGF\text{-}\beta^{high}IL\text{-}12_{p35}^{low}$ phenotypic polarization. Knocking down the expression of STAT3 resulted in the decreased p-STAT3 levels when IL-6 was added accordingly. Notably, the expression of IL-10 and TGF-β significantly decreased. However, the expression of $IL\text{-}12_{p35}$ restored when STAT3 was silenced in the IL-6-induced M2-like macrophages, which is also supported by previous report [22]. Hence, IL-6 negatively regulates $IL\text{-}12_{p35}$ expression through STAT3 pathway that promotes macrophages M2 differentiation. These results provide evidence that a high density of M2 macrophages infiltrating gastric cancer was induced by the high production of IL-6 via activating STAT3.

Furthermore, our study found that the production of IL-6 in gastric cancer tissues was correlated with tumor stages and a high production of IL-6-predicted poor prognosis of gastric cancer patients. This result is consistent with a previous report [31]. Increased IL-6 expression also predicts poor prognosis in oral squamous cell carcinoma [32] and head and neck squamous cell carcinoma [33]. The proliferation and migration abilities of gastric cancer cells co-cultured with M2-type macrophages' supernatant in vitro were significantly increased compared with the control group. However, neutralization of IL-10 or TGF-β by adding the antibodies to the M2 supernatants attenuated the pro-proliferation and pro-migration of M2 supernatants. This finding may explain why the high density of M2 macrophages infiltration in tumors, thus predicting a poor prognosis in our study and previous reports [34]. M2 macrophages produce IL-10 and TGF-β, leading to a suppression of general anti-tumor immune responses, promoting tumor neoangiogenesis by the secretion of pro-angiogenic factors, and defining the invasive microenvironment to facilitate tumor metastasis and dissemination [35]. It is now extensively acknowledged that M2-type macrophages have a significant effect on the tumor development and metastasis of many solid tumors, such as breast cancer [36, 37], pancreatic cancer [38], B cell lymphoma [39], and ovarian cancer [40]. The correlation

between M2 TAMs infiltration and poor survival has also been demonstrated in several other cancer types [38, 41, 42]. Therefore, IL-6 in tumor sites induces M2 macrophage differentiation and promotes M2 macrophage secretion of IL-10 and TGF-β and even other pro-tumor cytokines [22], thus favoring tumor growth and tumor metastasis in gastric cancer [43].

In conclusion, our data suggest that the increased production of IL-6 in tumor sites may play a major role in promoting M2 macrophage differentiation via activating STAT3 during GC establishment and progression. Therefore, blocking STAT3 activation may provide a new therapeutic direction for GC patients.

**Acknowledgements** We thank the Department of Pathology, Department of Blood Transfusion, Southwest Hospital, Third Military Medical University, Chongqing, China, for their excellent technical assistance. This work was supported by the National Key Research and Development Program of China (2016YFC1302200) and the National Natural Science Foundation of China (NSFC, No. 81372560).

**Compliance with ethical standards**

**Conflict of interest** The authors declare that they have no conflicts of interest.

## References

1. Condeelis J, Pollard JW (2006) Macrophages: obligate partners for tumor cell migration, invasion, and metastasis. Cell 124:263–266
2. Mantovani A, Sica A, Sozzani S, Allavena P, Vecchi A, Locati M (2004) The chemokine system in diverse forms of macrophage activation and polarization. Trends Immunol 25:677–686
3. Mosser DM (2003) The many faces of macrophage activation. J Leukoc Biol 73:209–212
4. Verreck FA, de Boer T, Langenberg DM et al (2004) Human IL-23-producing type 1 macrophages promote but IL-10-producing type 2 macrophages subvert immunity to (myco)bacteria. Proc Natl Acad Sci USA 101:4560–4565
5. Benoit M, Desnues B, Mege JL (2008) Macrophage polarization in bacterial infections. J Immunol 181:3733–3739
6. Mills CD, Kincaid K, Alt JM, Heilman MJ, Hill AM (2000) M-1/M-2 macrophages and the Th1/Th2 paradigm. J Immunol 164:6166–6173
7. Satoh T, Takeuchi O, Vandenbon A et al (2010) The Jmjd3-Irf4 axis regulates M2 macrophage polarization and host responses against helminth infection. Nat Immunol 11:936–944
8. Gordon S, Martinez FO (2010) Alternative activation of macrophages: mechanism and functions. Immunity 32:593–604
9. Mantovani A, Sozzani S, Locati M, Allavena P, Sica A (2002) Macrophage polarization: tumor-associated macrophages as a paradigm for polarized M2 mononuclear phagocytes. Trends Immunol 23:549–555
10. Ouchi N, Parker JL, Lugus JJ, Walsh K (2011) Adipokines in inflammation and metabolic disease. Nat Rev Immunol 11:85–97
11. Mauer J, Chaurasia B, Goldau J et al (2014) Signaling by IL-6 promotes alternative activation of macrophages to limit endotoxemia and obesity-associated resistance to insulin. Nat Immunol 15:423–430
12. Kraakman MJ, Kammoun HL, Allen TL et al (2015) Blocking IL-6 trans-signaling prevents high-fat diet-induced adipose tissue macrophage recruitment but does not improve insulin resistance. Cell Metab 21:403–416
13. Rohleder N, Aringer M, Boentert M (2012) Role of interleukin-6 in stress, sleep, and fatigue. Ann N Y Acad Sci 1261:88–96
14. Aoki Y, Feldman GM, Tosato G (2003) Inhibition of STAT3 signaling induces apoptosis and decreases survivin expression in primary effusion lymphoma. Blood 101:1535–1542
15. Azare J, Doane A, Leslie K et al (2011) Stat3 mediates expression of autotaxin in breast cancer. PLoS One 6:e27851
16. Xiong H, Zhang ZG, Tian XQ, Sun DF, Liang QC, Zhang YJ, Lu R, Chen YX, Fang JY (2008) Inhibition of JAK1, 2/STAT3 signaling induces apoptosis, cell cycle arrest, and reduces tumor cell invasion in colorectal cancer cells. Neoplasia 10:287–297
17. Leeman RJ, Lui VWY, Grandis JR (2006) STAT3 as a therapeutic target in head and neck cancer. Expert Opin Biol Ther 6:231–241
18. Mosser DM, Edwards JP (2008) Exploring the full spectrum of macrophage activation. Nat Rev Immunol 8:958–969
19. Spence S, Fitzsimons A, Boyd CR et al (2013) Suppressors of cytokine signaling 2 and 3 diametrically control macrophage polarization. Immunity 38:66–78
20. Zhuang Y, Peng LS, Zhao YL et al (2012) CD8(+) T cells that produce interleukin-17 regulate myeloid-derived suppressor cells and are associated with survival time of patients with gastric cancer. Gastroenterology 143:951–962
21. Hunter CA, Jones SA (2015) IL-6 as a keystone cytokine in health and disease. Nat Immunol 16:448–457
22. Duluc D, Delneste Y, Tan F et al (2007) Tumor-associated leukemia inhibitory factor and IL-6 skew monocyte differentiation into tumor-associated macrophage-like cells. Blood 110:4319–4330
23. Mantovani A, Allavena P, Sica A (2004) Tumour-associated macrophages as a prototypic type II polarised phagocyte population: role in tumour progression. Eur J Cancer 40:1660–1667
24. Sica A, Schioppa T, Mantovani A, Allavena P (2006) Tumour-associated macrophages are a distinct M2 polarised population promoting tumour progression: potential targets of anti-cancer therapy. Eur J Cancer 42:717–727
25. Hutchins AP, Poulain S, Miranda-Saavedra D (2012) Genome-wide analysis of STAT3 binding in vivo predicts effectors of the anti-inflammatory response in macrophages. Blood 119:E110–E119
26. Yan Y, Zhang J, Li JH, Liu X, Wang JZ, Qu HY, Wang JS, Duan XY (2016) High tumor-associated macrophages infiltration is associated with poor prognosis and may contribute to the phenomenon of epithelial–mesenchymal transition in gastric cancer. Onco Targets Ther 9:3975–3983
27. Yuan FJ, Fu X, Shi HF, Chen GP, Dong P, Zhang WY (2014) Induction of murine macrophage M2 polarization by cigarette smoke extract via the JAK2/STAT3 Pathway. PLoS One 9:e107063
28. Hasita H, Komohara Y, Okabe H, Masuda T, Ohnishi K, Lei XF, Beppu T, Baba H, Takeya M (2010) Significance of alternatively activated macrophages in patients with intrahepatic cholangiocarcinoma. Cancer Sci 101:1913–1919
29. Shiraishi D, Fujiwara Y, Komohara Y, Mizuta H, Takeya M (2012) Glucagon-like peptide-1 (GLP-1) induces M2 polarization of human macrophages via STAT3 activation. Biochem Biophys Res Commun 425:304–308
30. Gordon S (2003) Alternative activation of macrophages. Nat Rev Immunol 3:23–35
31. Necula LG, Chivu-Economescu M, Stanciulescu EL et al (2012) IL-6 and IL-11 as markers for tumor aggressiveness and prognosis in gastric adenocarcinoma patients without mutations in Gp130 subunits. J Gastrointest Liver Dis 21:23–29

32. Jinno T, Kawano S, Maruse Y et al (2015) Increased expression of interleukin-6 predicts poor response to chemoradiotherapy and unfavorable prognosis in oral squamous cell carcinoma. Oncol Rep 33:2161–2168
33. Gao J, Zhao S, Halstensen TS (2016) Increased interleukin-6 expression is associated with poor prognosis and acquired cisplatin resistance in head and neck squamous cell carcinoma. Oncol Rep 35:3265–3274
34. Lin CN, Wang CJ, Chao YJ, Lai MD, Shan YS (2015) The significance of the co-existence of osteopontin and tumor-associated macrophages in gastric cancer progression. BMC Cancer 15:128
35. Sica A, Larghi P, Mancino A et al (2008) Macrophage polarization in tumour progression. Semin Cancer Biol 18:349–355
36. Oghumu S, Varikuti S, Terrazas C, Kotov D, Nasser MW, Powell CA, Ganju RK, Satoskar AR (2014) CXCR3 deficiency enhances tumor progression by promoting macrophage M2 polarization in a murine breast cancer model. Immunology 143:109–119
37. Tiainen S, Tumelius R, Rilla K, Hamalainen K, Tammi M, Tammi R, Kosma V-M, Oikari S, Auvinen P (2015) High numbers of macrophages, especially M2-like (CD163-positive), correlate with hyaluronan accumulation and poor outcome in breast cancer. Histopathology 66:873–883
38. Hu H, Hang J-J, Han T, Zhuo M, Jiao F, Wang L-W (2016) The M2 phenotype of tumor-associated macrophages in the stroma confers a poor prognosis in pancreatic cancer. Tumor Biol 37:8657–8664
39. Shen L, Li H, Shi Y, Wang D, Gong J, Xun J, Zhou S, Xiang R, Tan X (2016) M2 tumour-associated macrophages contribute to tumour progression via legumain remodelling the extracellular matrix in diffuse large B cell lymphoma. Sci Rep 6:30347
40. Lan C, Huang X, Lin S, Huang H, Cai Q, Wan T, Lu J, Liu J (2013) Expression of M2-polarized macrophages is associated with poor prognosis for advanced epithelial ovarian cancer. Technol Cancer Res Treat 12:259–267
41. Ryder M, Ghossein RA, Ricarte-Filho JCM, Knauf JA, Fagin JA (2008) Increased density of tumor-associated macrophages is associated with decreased survival in advanced thyroid cancer. Endocr Relat Cancer 15:1069–1074
42. Niino D, Komohara Y, Kimura Y et al (2010) Ratio of M2 macrophage expression is closely associated with poor prognosis for Angioimmunoblastic T-cell lymphoma (AITL). Pathol Int 60:278–283
43. Wang ZG, Si XL, Xu A et al (2013) Activation of STAT3 in human gastric cancer cells via interleukin (IL)-6-type cytokine signaling correlates with clinical implications. PLoS One 8:e75788